Pergamon

Int. J. Heat Mass Transfer. Vol. 41, No. 1, pp. 11–23, 1998

Printed in Great Britain
0017-9310/98 $19.00+0.00

PII: S0017-9310(97)00114-2

Free convection driven by an exothermic reaction on a vertical surface embedded in porous media

B. J. MINTO
Centre for Computational Fluid Dynamics, University of Leeds, Leeds LS2 9JT, U.K.

D. B. INGHAM†
Department of Applied Mathematical Studies, University of Leeds, Leeds LS2 9JT

and

I. POP
Faculty of Mathematics, University of Cluj, R3400, Cluj, Romania

(*Received* 22 *April* 1997)

Abstract—The free-convection boundary-layer flow on a vertical surface embedded in a porous media driven by an exothermic catalytic chemical reaction on the surface is considered. The governing equations of this flow are reduced to a pair of coupled, parabolic partial differential equations for the temperature and the concentration of the fluid reactant. These equations are governed by the dimensionless chemical parameters λ and ε, which are measures of the reactant consumption and the activation energy, respectively, as well as the Lewis number. Similarity solutions are obtained which are valid near the leading edge of the surface. Asymptotic solutions, which are valid at large distances downstream from the leading edge, are obtained for the two independent situations when $\lambda = 0$ and $\lambda \neq 0$. A numerical solution to the partial differential equations is then obtained. The numerical solution is investigated for a range of the chemical parameters λ and ε, and was found to exhibit localized rapid increases in temperature when λ and ε are small. Comparisons between the numerical solution and the similarity and asymptotic solutions are made and are found to be in good agreement. © 1997 Elsevier Science Ltd.

1. INTRODUCTION

Convective flow in a porous media occurs widely in natural phenomena and industrial applications, such as geothermal energy extraction, oil recovery, food processing, casting and welding of a manufacturing process, the dispersion of chemical contaminants in various processes in the chemical industry and in the environment, to name but a few. This topic is of vital importance to these systems, thereby generating the need for a full understanding of this process. A detailed review of the subject, including an exhaustive list of references, was recently performed by Nield and Bejan [1].

Free convection boundary-layer flow in porous media along a vertical flat plate was first considered by Cheng and Minkowycz [2], but their analysis has since been refined and generalized. In all previous studies, it has been assumed that the heat transfer process occurs by heating or cooling the surface of the plate. However, the free convection boundary-layer flow along a vertical surface surrounded by a fluid-saturated porous medium driven by a catalytic surface heating can be of importance for the design of equipment used in several types of engineering systems. Within the field of chemical engineering and the petrochemical industries the interaction between chemical reaction and free convection occurs widely. Areas of research include tubular laboratory reactors, chemical vapour deposition systems, the oxidation of solid materials in large containers, the synthesis of ceramic materials by a self-propagating reaction, combustion in underground reservoirs for enhanced oil recovery and the reduction of hazardous combustion products using catalytic porous beds, amongst others.

The theme of chemically reactive flow in porous media has received relatively little attention until recently. Kordylewski and Krajewski [3], and Viljonen and Hlavacek [4], studied the chemically reacting flow in porous media at low temperatures. The premixed combustion in porous media was treated by Chen *et al.* [5], while Hsu *et al.* [6] studied a similar problem using detailed chemical kinetics, and the

† Author to whom correspondence should be addressed.

NOMENCLATURE

A	reactant species
B	product species
C	concentration of reactant A
D	mass diffusivity
E	activation energy of the reactant
$f, \hat{f}, F$	reduced streamfunction profiles
g	magnitude of the gravitational acceleration
h	reduced concentration profile
k_0	constant
k_m	effective thermal conductivity of the porous medium
K	permeability
L	reaction length scale
Le	Lewis number
Q	heat of reaction
R	universal gas constant
Ra	Rayleigh number
T	temperature
T_R	temperature scaling
u, v	non-dimensional velocity components along the x- and y-axes, respectively
U_R	vertical velocity scaling
x, y	non-dimensional co-ordinates perpendicular and normal to the surface, respectively.

Greek symbols

α_m	effective thermal diffusivity of the porous medium
β	thermal expansion coefficient
γ	constant
ε	activation energy parameter
Φ	non-dimensional concentration of the reactant A
η, ζ, ξ	similarity variables
λ	reactant consumption parameter
υ	kinematic viscosity
θ	non-dimensional temperature
ψ	non-dimensional streamfunction.

Subscripts

w	wall condition
∞	ambient condition.

Superscripts

$\bar{}$	dimensional variable
$'$	differentiation with respect to a similarity variable.

effects of varying the porous material used, the burner geometry, and the values of the governing kinetic parameters. Chao *et al.* [7] analyzed the nonpremixed burning of a condensed fuel in a porous medium with a natural convective oxidizer flow adjacent to the wall and obtained a solution for the flame temperature, the stand-off distance and the mass consumption rate. Recently, Chao *et al.* [8] investigated theoretically the heat transfer and reaction characteristics of a chemically reactive forced convection flow near the stagnation point of a catalytic porous bed with finite thickness. A single-reactant, first-order, one-step Arrhenius reaction is assumed to occur. By considering the flow in this manner allowed the continuity and momentum equations to be decoupled from the energy and species equations, so that only the latter need be solved. The steady state and initial transient period in the gas phase upstream and in the catalytic porous bed were investigated using both perturbation and finite-difference methods.

The interaction between the free convection boundary-layer flow of a pure, viscous fluid near a stagnation point and along a heated vertical surface was only recently documented by Chaudhary and Merkin [9], and Merkin and Chaudhary [10]. According to these authors, there is a three-way coupling between fluid flow, fluid/surface temperatures and reactant species concentration. Thus, the interaction between the homogeneous reactions in the bulk of the fluid and the heterogeneous reactions occurring on a catalytic surface is very complex and, therefore, difficult to model.

In this paper, a theoretical analysis is considered of the steady free convection along a vertical flat surface embedded in a fluid-saturated porous medium, where the flow is driven by catalytic surface heating. The model and flow configuration have as their starting point the work by Merkin and Chaudhary [10]. We assume that the flow in the boundary-layer is driven purely by free convection and consider only heterogeneous reactions, i.e. we assume that reaction takes place only on the catalytic surface and can be represented schematically by the single first-order Arrhenius kinetics. Also, the standard Darcy–Boussinesq approximation is evoked, thereby simplifying the flow under consideration. The conservation equations reduce to a system of two coupled partial differential equations for the dimensionless temperature and the dimensionless concentration. This pair of partial differential equations is characterized by three parameters: the reactant consumption parameter, λ, the activation energy parameter, ε, and the Lewis number, Le. First, similarity solutions are obtained, which are valid near the leading edge of the surface,

and these are then continued downstream by numerically solving the full boundary-layer equations, generating numerical solutions valid for all possible values of ε and λ. Asymptotic solutions which are valid at large distances downstream of the leading edge, were then obtained. Throughout this paper the Lewis number is consistently taken as unity.

2. BASIC EQUATIONS

We consider a catalytic surface, with co-ordinates $\bar{x}$ and $\bar{y}$ measuring the distance parallel and perpendicular to the surface, which is embedded in the porous media at an ambient temperature T_∞. It is assumed, according to Nield and Bejan [1, pp. 34–35] and Merkin and Chaudhary [9, 10], that a reaction takes place only on the surface, which can be represented schematically by a single first-order, exothermic reaction governed by Arrhenius kinetics, namely:

$$A \to B \quad D\frac{\partial C}{\partial \bar{y}} = k_0 C \exp\left(-\frac{E}{RT}\right) \tag{1}$$

where C is the concentration of the reactant A, T is the fluid temperature, B is the product species, D is the mass diffusivity, k_0 is a known constant, E is the activation energy and R is the universal gas constant. It is also assumed that no further reaction takes place in the fluid-saturated porous media and that at large distances from the surface the concentration of the reactant A is uniform at a value C_∞. Heat is released from the surface by the reaction at a rate

$$k_m \frac{\partial T}{\partial \bar{y}} = -Qk_0 C \exp\left(-\frac{E}{RT}\right) \tag{2}$$

where Q is the heat of reaction and k_m is the thermal conductivity of the porous medium. This heat is taken from the surface into the porous media by conduction and thus a free convection flow is set up.

Assuming that the porous medium is isotropic and homogeneous and that the fluid is incompressible, we invoke the Darcy–Boussinesq approximation to obtain the governing equations

$$\frac{\partial \bar{u}}{\partial \bar{x}} + \frac{\partial \bar{v}}{\partial \bar{y}} = 0 \tag{3}$$

$$\bar{u} = \frac{g\beta K}{\upsilon}(T - T_\infty) \tag{4}$$

$$\bar{u}\frac{\partial T}{\partial \bar{x}} + \bar{v}\frac{\partial T}{\partial \bar{y}} = \alpha_m \frac{\partial^2 T}{\partial \bar{y}^2} \tag{5}$$

$$\bar{u}\frac{\partial C}{\partial \bar{x}} + \bar{v}\frac{\partial C}{\partial \bar{y}} = D\frac{\partial^2 C}{\partial \bar{y}^2} \tag{6}$$

which have to be solved, subject to the appropriate boundary conditions, given by

$$\bar{v} = 0, \quad k_m \frac{\partial T}{\partial \bar{y}} = -Qk_0 C \exp\left(-\frac{E}{RT}\right)$$

$$D\frac{\partial C}{\partial \bar{y}} = k_0 C \exp\left(-\frac{E}{RT}\right) \quad \text{on } \bar{y} = 0 \quad \bar{x} > 0 \tag{7a}$$

$$\bar{u} \to 0 \quad T \to T_\infty \quad C \to C_\infty \quad \text{as } \bar{y} \to \infty \quad \bar{x} > 0 \tag{7b}$$

$$\bar{u} = 0 \quad \bar{v} = 0 \quad T = T_\infty \quad C = C_\infty \quad \text{on } \bar{x} = 0 \quad \bar{y} > 0 \tag{7c}$$

where $(\bar{u}, \bar{v})$ are the velocity components in the $(\bar{x}, \bar{y})$ directions. In equations (3)–(7), g is the magnitude of the gravitational acceleration, β is the coefficient of thermal expansion, K is the permeability of the porous media, υ is the kinematic viscosity of the fluid and α_m is the effective thermal diffusivity of the porous media. We now introduce the following non-dimensional variables

$$x = \frac{\bar{x}}{L} \quad y = Ra^{1/2}\left(\frac{\bar{y}}{L}\right) \quad u = \frac{\bar{u}}{U_R} \quad v = Ra^{1/2}\left(\frac{\bar{v}}{L}\right)$$

$$\theta = \frac{(T - T_\infty)}{T_R} \quad \Phi = \frac{C}{C_\infty} \tag{8}$$

where T_R, U_R are the scalings for the temperature and velocity, L is the 'reaction length scale' and Ra is the Rayleigh number, defined as

$$T_R = \frac{RT_\infty^2}{E} \quad U_R = \frac{g\beta K T_R}{\upsilon}$$

$$L = \frac{U_R k_R^2 T_R^2}{\alpha_m Q^2 k_0^2 C_\infty^2} \exp\left(\frac{2E}{RT_\infty}\right) \quad Ra = \frac{\rho g \beta K T_R L}{\alpha_m \mu}. \tag{9}$$

Equation (3) enables a non-dimensional stream-function ψ to be defined such that $u = \partial\psi/\partial y$ and $v = -\partial\psi/\partial x$. Thus, equations (4)–(6) can be written in the form

$$\theta = \frac{\partial \Psi}{\partial y} \tag{10}$$

$$\frac{\partial \Psi}{\partial y}\frac{\partial \theta}{\partial x} - \frac{\partial \Psi}{\partial x}\frac{\partial \theta}{\partial y} = \frac{\partial^2 \theta}{\partial y^2} \tag{11}$$

$$\frac{\partial \Psi}{\partial y}\frac{\partial \Phi}{\partial x} - \frac{\partial \Psi \partial \Phi}{\partial x \partial y} = \frac{1}{Le}\frac{\partial^2 \Phi}{\partial y^2} \tag{12}$$

where $Le = \alpha_m/D$ is the Lewis number. The boundary conditions (7) now become

$$\psi = 0 \quad \frac{\partial \theta}{\partial y} = -\Phi \exp\left(\frac{\theta}{1 + \varepsilon\theta}\right)$$

$$\frac{\partial \Phi}{\partial y} = \lambda \Phi \exp\left(\frac{\theta}{1 + \varepsilon\theta}\right) \quad \text{on } y = 0 \quad x > 0 \tag{13a}$$

$$\frac{\partial \Psi}{\partial y} \to 0 \quad \theta \to 0 \quad \Phi \to 1 \quad \text{as } y \to \infty \quad x > 0 \tag{13b}$$

$$\Psi = 0 \quad \theta = 0 \quad \Phi = 1 \quad \text{on } x = 0 \quad y > 0 \tag{13c}$$

where λ and ε are a measure of the reactant consumption and activation energy, respectively, and are given by

$$\lambda = \frac{k_R R T_\infty^2}{QDEC_\infty} \quad \varepsilon = \frac{RT_\infty}{E}. \tag{14}$$

3. SOLUTION VALID NEAR TO THE LEADING EDGE OF THE CATALYTIC SURFACE, IE SMALL *x*

The flow develops initially by heat transfer due to a constant wall flux from the surface, which suggests the transformation

$$\psi = x^{2/3} f(x,\eta) \quad \theta = x^{1/3} \frac{\partial f}{\partial \eta} \quad \Phi = h(x,\eta) \quad \eta = \frac{y}{x^{1/3}} \tag{15}$$

to obtain a solution of equations (11) and (12) which is valid near to the leading edge of the catalytic surface. On applying the transformation (15) to equations (11) and (12) and their associated boundary conditions (13) we obtain

$$\frac{\partial^3 f}{\partial \eta^3} + \frac{2}{3} f \frac{\partial^2 f}{\partial \eta^2} - \frac{1}{3}\left(\frac{\partial f}{\partial \eta}\right)^2 = x\left(\frac{\partial f}{\partial \eta}\frac{\partial^2 f}{\partial x \partial \eta} - \frac{\partial f}{\partial x}\frac{\partial^2 f}{\partial \eta^2}\right) \tag{16}$$

$$\frac{1}{Le}\frac{\partial^2 h}{\partial \eta^2} + \frac{2}{3} f \frac{\partial h}{\partial \eta} = x\left(\frac{\partial f}{\partial \eta}\frac{\partial h}{\partial x} - \frac{\partial f}{\partial x}\frac{\partial h}{\partial \eta}\right) \tag{17}$$

which have to be solved subject to the boundary conditions

$$f = 0, \quad \frac{\partial^2 f}{\partial \eta^2} = -h \exp\left(\frac{x^{1/3}\dfrac{\partial f}{\partial \eta}}{1 + \varepsilon x^{1/3}\dfrac{\partial f}{\partial \eta}}\right)$$

$$\frac{\partial h}{\partial \eta} = \lambda x^{1/3} h \exp\left(\frac{x^{1/3}\dfrac{\partial f}{\partial \eta}}{1 + \varepsilon x^{1/3}\dfrac{\partial f}{\partial \eta}}\right) \quad \text{on } \eta = 0 \tag{18a}$$

$$\frac{\partial f}{\partial \eta} \to 0, \quad h \to 1 \quad \text{as } \eta \to \infty. \tag{18b}$$

The form of the boundary conditions (18) suggest that the consistent forms of expansion for $f(x,\eta)$ and $h(x,\eta)$ are

$$f(x,\eta) = f_0(\eta) + x^{1/3} f_1(\eta) + \ldots \tag{19a}$$

$$h(x,\eta) = h_0(\eta) + x^{1/3} h_1(\eta) + \ldots \tag{19b}$$

where at the leading order, $\mathbf{O}(x^{1/3})^0$, the coefficient functions satisfy the ordinary differential equations

$$f_0''' + \frac{2}{3} f_0 f_0'' - \frac{1}{3}(f_0')^2 = 0, \quad \frac{1}{Le} h_0'' + \frac{2}{3} f_0 h_0' = 0 \tag{20a}$$

which have to be solved subject to the boundary conditions

$$f_0(0) = 0, \quad f_0''(0) = -h_0(0), \quad h_0'(0) = 0,$$
$$f_0'(\infty) = 0, \quad h_0(\infty) = 1. \tag{20b}$$

At the second-order, $\mathbf{O}(x^{1/3})^1$, the coefficient functions satisfy the ordinary differential equations

$$f_0''' + \frac{2}{3} f_0 f_1'' - f_0' f_1' + f_0'' f_1' + f_0'' f_1 = 0$$

$$\frac{1}{Le} h_1'' + \frac{2}{3} f_0 h_1' - \frac{1}{3} f_0' h_1 + f_1 h_0'' = 0 \tag{21a}$$

which have to be solved subject to the boundary conditions

$$f_1(0) = 0 \quad f_1''(0) = -h_1(0) - h_0(0) f_0'(0)$$
$$h_1'(0) = \lambda h_0(0) \quad f_1'(\infty) = 0 \quad h_1(\infty) = 0 \tag{21b}$$

where the primes used denote differentiation with respect to η. The equation for h_0 has only the trivial solution

$$h_0(\eta) \equiv 1. \tag{22}$$

On considering equation (22), equation (20a) for f_0 is now in the form satisfying the standard free convection problem for constant wall heat flux, which is well documented in the literature [11–13]. Thus, from Rees and Pop [12], we have

$$f_0'(0) = 1.29618. \tag{23}$$

At the second-order, $\mathbf{O}(x^{1/3})^1$, we write

$$f_1 = (f_0'(0) + \lambda \tilde{h}_1(0))\tilde{f}_1(\eta) \quad h_1 = \lambda \tilde{h}_1(\eta) \tag{24}$$

to eliminate λ from equation (21). On applying transformation (24) to equation (21a) and their associated boundary conditions (21b) we obtain

$$\tilde{f}_1''' + \frac{2}{3} f_0 \tilde{f}_1'' - f_0' \tilde{f}_1' + f_0'' \tilde{f}_1' + f_0'' \tilde{f}_1 = 0$$

$$\frac{1}{Le}\tilde{h}_1'' + \frac{2}{3} f_0 \tilde{h}_1' - \frac{1}{3} f_0' \tilde{h}_1 = 0 \tag{25a}$$

which have to be solved subject to the boundary conditions

$$\tilde{f}_1(0) = 0 \quad \tilde{f}_1''(0) = -1 \quad \tilde{h}_1'(0) = 1$$
$$\tilde{f}_1'(\infty) = 0 \quad \tilde{h}_1(\infty) = 0. \tag{25b}$$

Thus, from equations (15), (19) and (24), we can obtain expressions for the dimensionless wall temperature, $\theta(x,0) = \theta_w(x)$ and the dimensionless surface concentration, $\Phi(x,0) = \Phi_w(x)$, in the form

$$\theta_w(x) = x^{1/3}\{f_0'(0) + x^{1/3}(f_0'(0) + \lambda\tilde{h}_1(0))\tilde{f}_1'(0) + \ldots\} \quad (26a)$$

$$\Phi_w(x) = 1 + \tilde{h}_1(0)\lambda x^{1/3} + \ldots. \quad (26b)$$

On solving numerically equations (25), utilizing the NAG routine D02GAF, for the case when Le is taken as unity, we can determine the values of $\tilde{f}_1(0)$ and $\tilde{h}_1(0)$. A value for $f_0'(0)$ was also determined, by solving equations (20) and this was found to be in agreement with the value given in relation (23), as determined in [12]. It now follows from equations (10)–(13) that, for the case when $Le = 1$,

$$\Phi(x, y) = 1 - \lambda\theta(x, y). \quad (27)$$

In this case, equations (19) and (27) give $\tilde{h}_1(0) = -f_0'(0)$ so that the expressions (26), together with the numerical results for $f_0'(0)$ and $\tilde{f}_1(0)$ become

$$\theta_w(x) = 1.29618x^{1/3}\{1 + 0.73429x^{1/3}(1-\lambda) + \ldots\} \quad (28a)$$

$$\Phi_w(x) = 1 - 0.73429\lambda x^{1/3} + \ldots \quad (28b)$$

which are only valid for cases where $x \ll 1$.

4. SOLUTION VALID FAR FROM THE LEADING EDGE OF THE CATALYTIC SURFACE, IE LARGE x

Taking the values of the reactant consumption parameter as $\lambda = 0$ ($\varepsilon \neq 0$) or $\lambda \neq 0$ in equations (16)–(18) leads to two essentially distinct types of asymptotic behaviours. It is this aspect that we next discuss, starting with the asymptotic solution for the case when $\lambda = 0$.

4.1. *Reactant consumption neglected*, $\lambda = 0$, $\varepsilon \neq 0$

On taking $\lambda = 0$, i.e. equation (27) implies that $\Phi(x, y) \equiv 1$, we can see that the transformation variables (15) are again appropriate to deal with equations (10)–(13), in order to obtain a solution valid for large x. The form of the boundary conditions (18) suggest that the consistent form of expansion for $f(x, \eta)$ is

$$f(x, \eta) = \hat{f}_0(\eta) + x^{-1/3}\hat{f}_1(\eta) + \ldots \quad (29)$$

where at the leading order, $\mathbf{O}(x^{-1/3})^0$, the coefficient functions satisfy the ordinary differential equations

$$\hat{f}_0''' + \tfrac{2}{3}\hat{f}_0\hat{f}_0'' - \tfrac{1}{3}(\hat{f}_0')^2 = 0 \quad (30a)$$

which have to be solved subject to the boundary conditions

$$\hat{f}_0(0) = 0 \quad \hat{f}_0''(0) = -\exp\left(\frac{1}{\varepsilon}\right) \quad \hat{f}_0'(\infty) = 0. \quad (30b)$$

At the second order, $\mathbf{O}(x^{-1/3})^1$, the coefficient functions satisfy the ordinary differential equations

$$\hat{f}_1''' + \tfrac{2}{3}\hat{f}_0\hat{f}_1'' - \tfrac{1}{3}\hat{f}_0'\hat{f}_1' + \tfrac{1}{3}\hat{f}_0''\hat{f}_1 = 0 \quad (31a)$$

$$\hat{f}_1(0) = 0 \quad \hat{f}_1''(0) = \frac{1}{\varepsilon^2}\exp\left(\frac{1}{\varepsilon}\right)[\hat{f}_0'(0)]^{-1} \quad \hat{f}_1'(\infty) = 0 \quad (31b)$$

where the primes denote differentiation with respect to η. To simplify the form of the boundary conditions (30b) and (31b) we introduce uniform wall heat-flux variables of the form:

$$\hat{f}_0 = \left(\exp\left(\frac{1}{\varepsilon}\right)\right)^{1/3}\bar{f}_0(\bar{\eta})$$

$$\hat{f}_1 = \frac{1}{\varepsilon^2}\left(\exp\left(\frac{1}{\varepsilon}\right)\right)^{-1/3}\bar{f}_1(\bar{\eta})$$

$$\eta = \left(\exp\left(\frac{1}{\varepsilon}\right)\right)^{-1/3}\bar{\eta} \quad (32)$$

which has the effect of leaving the form of equations (30a) and (31a) unchanged, whilst the boundary conditions (30b) and (31b) now become

$$\bar{f}_0(0) = 0 \quad \bar{f}_0''(0) = -1 \quad \bar{f}_0'(\infty) = 0 \quad (33a)$$

$$\bar{f}_1(0) = 0 \quad \bar{f}_1''(0) = [\bar{f}_0'(0)]^{-1} \quad \bar{f}_1'(\infty) = 0 \quad (33b)$$

where the primes now denote differentiation with respect to $\bar{\eta}$. Expressions for the dimensionless wall temperature and the dimensionless surface concentration are now obtained from equations (15), (29) and (32), in the form

$$\theta_w(x) = x^{1/3}\left(\exp\left(\frac{1}{\varepsilon}\right)\right)^{2/3} \times \left\{\bar{f}_0'(0) + \bar{f}_1'(0)\left(\exp\left(\frac{1}{\varepsilon}\right)\right)^{-2/3}\varepsilon^{-2}x^{-1/3} + \ldots\right\} \quad (34a)$$

$$\Phi_w(x) \equiv 1. \quad (34b)$$

On numerically solving equations (30a) and (31a), subject to the boundary conditions (33), again by implementing the NAG routine D02GAF for the case when $Le = 1$, values for $\bar{f}_0'(0)$ and $\bar{f}_1'(0)$ were obtained. As a result of this, expression (34) is now to be expressed as

$$\theta_w(x) = x^{1/3}\left(\exp\left(\frac{1}{\varepsilon}\right)\right)^{2/3} \times \left\{1.29618 - 0.85333\left(\exp\left(\frac{1}{\varepsilon}\right)\right)^{-2/3}\varepsilon^{-2}x^{-1/3} + \ldots\right\} \quad (35a)$$

$$\Phi_w(x) \equiv 1 \quad (35b)$$

which are only valid for cases where $x \gg 1$, and do not hold for cases where $\varepsilon = 0$.

4.2. *Reactant consumption included,* $\lambda \neq 0$

For the case when $\lambda \neq 0$, we assume that the dimensionless wall temperature, θ_w, approaches a constant value and that the dimensionless surface concentration, Φ_w, tends towards zero as the distance along the surface, x, tends towards infinity. To this end the transformation variables (15), previously applied to equations (10)–(13), are dropped in favour of a transformation reflecting the development of the flow away from the leading edge of the surface, influenced by convection. The suggested transformation is of the form

$$\psi = x^{1/2}F(x,\zeta) \quad \theta = \frac{\partial F}{\partial \zeta} \quad \Phi = \Phi(x,\zeta) \quad \zeta = \frac{y}{x^{1/2}}. \tag{36}$$

On applying the transformation (37) to equations (11) and (12) and their associated boundary conditions (13) we obtain

$$\frac{\partial^3 F}{\partial \zeta^3} + \frac{1}{2}F\frac{\partial^2 F}{\partial \zeta^2} = x\left(\frac{\partial F}{\partial \zeta}\frac{\partial^2 F}{\partial x \partial \zeta} - \frac{\partial F}{\partial x}\frac{\partial^2 F}{\partial \zeta^2}\right) \tag{37}$$

$$\frac{1}{Le}\frac{\partial^2 \Phi}{\partial \zeta^2} + \frac{1}{2}F\frac{\partial \Phi}{\partial \zeta} = x\left(\frac{\partial F}{\partial \zeta}\frac{\partial \Phi}{\partial x} - \frac{\partial F}{\partial x}\frac{\partial \Phi}{\partial \zeta}\right) \tag{38}$$

which have to be solved subject to the boundary conditions

$$F = 0, \quad \frac{\partial^2 F}{\partial \zeta^2}x^{-1/2} = -\Phi \exp\left(\frac{\dfrac{\partial F}{\partial \zeta}}{1+\varepsilon\dfrac{\partial F}{\partial \zeta}}\right)$$

$$\frac{\partial \Phi}{\partial \zeta}x^{-1/2} = \lambda\Phi \exp\left(\frac{\dfrac{\partial F}{\partial \zeta}}{1+\varepsilon\dfrac{\partial F}{\partial \zeta}}\right) \quad \text{on } \zeta = 0 \tag{39a}$$

$$\frac{\partial F}{\partial \zeta} \to 0, \quad \Phi \to 1 \quad \text{as } \zeta \to \infty. \tag{39b}$$

The form of the boundary conditions (39) suggest that the consistent forms of expansion for $F(x,\zeta)$ and $\Phi(x,\zeta)$ are

$$F(x,\zeta) = F_0(\zeta) + x^{-1/2}F_1(\zeta) + \ldots \tag{40a}$$

$$\Phi(x,\zeta) = \Phi_0(\zeta) + x^{-1/2}\Phi_1(\zeta) + \ldots \tag{40b}$$

where at the leading order, $\mathbf{O}(x^{-1/2})^0$, the coefficient functions satisfy the ordinary differential equations

$$F_0''' + \frac{1}{2}F_0F_0'' = 0 \quad \frac{1}{Le}\Phi_0'' + \frac{1}{2}F_0\Phi_0' = 0 \tag{41a}$$

which have to be solved subject to the boundary conditions

$$F_0(0) = 0 \quad \Phi_0(0) = 0 \quad F_0'(\infty) = 0 \quad \Phi_0(\infty) = 1 \tag{41b}$$

where the primes used denote differentiation with respect to ζ. Equation (41a) is the classical equation for the free convection boundary-layer flow on an isothermal vertical plate embedded in porous media, as described in ref. [2]. At this stage of the analysis the form of the boundary conditions (39a) make a value for $F_0'(0)$ indeterminable, due to the repeated boundary condition for $\Phi_0(0)$ and, therefore, we now consider the ordinary differential equations which the coefficient functions of equation (40) satisfies at the second-order, $\mathbf{O}(x^{-1/2})^1$, namely the equations

$$F_1''' + \frac{1}{2}F_0F_1'' + \frac{1}{2}F_0'F_1' = 0$$

$$\frac{1}{Le}\Phi_1'' + \frac{1}{2}F_0\Phi_1' + \frac{1}{2}F_0'\Phi_1 = 0 \tag{42a}$$

which have to be solved subject to the boundary conditions

$$F_1(0) = 0 \quad \Phi_1(0) = -F_0''(0)\exp\left(\frac{-F_0'(0)}{1+\varepsilon F_0'(0)}\right)$$

$$\Phi_1(0) = \lambda^{-1}\Phi_0'(0)\exp\left(\frac{-F_0'(0)}{1+\varepsilon F_0'(0)}\right)$$

$$F_1'(\infty) = 0 \quad \Phi_1(\infty) = 0. \tag{42b}$$

Now to ensure consistency between the boundary conditions (42b), we enforce the condition

$$\lambda F_0''(0) + \Phi_0'(0) = 0 \tag{43}$$

and likewise for consistency between the boundary conditions (39a) at $\mathbf{O}(x^{-1/2})^2$, we enforce the condition

$$\lambda F_1''(0) + \Phi_1'(0) = 0. \tag{44}$$

Equations (43) and (44) now complete the sets of boundary conditions for the leading order and the second-order ordinary differential equations, given by equations (41a) and (42a), respectively. As before, we now introduce a transformation, to simplify the form of boundary conditions (42b), of the form

$$F_0 = (\lambda)^{-1/2}\bar{F}_0(\bar{\zeta}) \quad \Phi_0 = \bar{\Phi}_0(\bar{\zeta}) \quad F_1 = (\lambda)^{-2}\gamma\bar{F}_1(\bar{\zeta})$$

$$\Phi_1 = (\lambda)^{-3/2}\gamma\bar{\Phi}_1(\bar{\zeta}) \quad \bar{\zeta} = (\lambda)^{-1/2}\zeta \tag{45}$$

where γ is a constant given by

$$\gamma = \exp\left(-\frac{F_0'(0)}{1+\varepsilon F_0'(0)}\right). \tag{46}$$

On applying the transformation (45) to equations (41a) and (42a) and their associated boundary conditions we obtain

$$\bar{F}_0''' + \frac{1}{2}\bar{F}_0\bar{F}_0'' = 0 \quad \frac{1}{Le}\bar{\Phi}_0'' + \frac{1}{2}\bar{F}_0\bar{\Phi}_0' = 0 \tag{47a}$$

which have to be solved subject to the boundary conditions

$$\bar{F}_0(0) = 0 \quad \bar{\Phi}_0(0) = 0 \quad \bar{F}_0''(0) + \bar{\Phi}_0'(0) = 0$$

$$\bar{F}_0'(\infty) = 0 \quad \bar{\Phi}_0(\infty) = 1 \tag{47b}$$

and

$$\bar{F}_1''' + \frac{1}{2}\bar{F}_0\bar{F}_1'' + \frac{1}{2}\bar{F}_0'\bar{F}_1' = 0$$

$$\frac{1}{Le}\bar{\Phi}_1'' + \frac{1}{2}\bar{F}_0\bar{\Phi}_1' + \frac{1}{2}\bar{F}_0'\bar{\Phi}_1 = 0 \tag{48a}$$

which have to be solved subject to the boundary conditions

$$\bar{F}_1(0) = 0 \quad \bar{\Phi}_1(0) = \Phi_0'(0) \quad \bar{F}_1''(0) + \bar{\Phi}_1'(0) = 0$$

$$\bar{F}_1'(\infty) = 0 \quad \bar{\Phi}_1(\infty) = 0 \tag{48b}$$

where the primes now denote differentiation with respect to $\bar{\zeta}$. Expressions for the dimensionless wall temperature and the dimensionless surface concentration are now obtained from equations (36), (40) and (45), in the form

$$\theta_w(x) = (\lambda)^{-1}\left\{\bar{F}_0'(0) + \bar{F}_1'(0)(\lambda)^{-3/2} \times \exp\left(-\frac{\bar{F}_0'(0)}{\lambda + \varepsilon\bar{F}_0'(0)}\right)x^{-1/2} + \ldots\right\} \tag{49a}$$

$$\Phi_w(x) = \bar{\Phi}_0'(0)(\lambda)^{-3/2} \times \exp\left(-\frac{\bar{F}_0'(0)}{\lambda + \varepsilon\bar{F}_0'(0)}\right)x^{-1/2} + \ldots. \tag{49b}$$

On numerically solving equations (47a) and (48a) subject to the boundary conditions (47b) and (48b), respectively, again by implementing the NAG routine D02GAF for the case when $Le = 1$, values for $\bar{F}_0'(0)$, $\bar{\Phi}_0'(0)$ and $\bar{F}_1'(0)$ were obtained. For this case it can be noted, as described in ref. [2], that $\bar{F}_0'(0) \equiv 1$ and that $\bar{F}_1'(0) \equiv -\bar{\Phi}_0'(0)$. As a result of this, expression (49) is now expressed as

$$\theta_w(x) = (\lambda)^{-1}\left\{1 - 0.44375(\lambda)^{-3/2} \times \exp\left(-\frac{1}{\lambda + \varepsilon}\right)x^{-1/2} + \ldots\right\} \tag{50a}$$

$$\Phi_w(x) = 0.44375(\lambda)^{-3/2}\exp\left(-\frac{1}{\lambda + \varepsilon}\right)x^{-1/2} + \ldots \tag{50b}$$

which are only valid for cases where $x \gg 1$, and do not hold for the cases where $\lambda = 0$, as discussed in Section 3.1. As initially assumed at the beginning of this section it is clear from equations (50) that the dimensionless wall temperature tends towards a constant value, i.e. $\theta_w(x) \to (\lambda)^{-1}$ and that the dimensionless surface concentration tends towards zero, i.e. $\Phi_w(x) \to 0$, as $x \to \infty$.

5. NUMERICAL SOLUTION

The dimensionless wall temperature and the dimensionless surface concentration solutions which are valid near to and far from the leading edge of the catalytic surface, as derived in Sections 3 and 4, respectively, are now complemented by a numerical solution of the governing equations (10)–(13), thereby providing a smooth transition between the similarity and asymptotic solutions.

In Section 3, we found that the solution which is valid near to the leading edge of the catalytic surface developed in powers of $x^{1/3}$ and, therefore, there exists a singularity at the leading edge of the surface, i.e. at $x = 0$. A similar problem was solved numerically by Mahmood and Merkin [8], where they proposed the use of a finite-difference scheme, where the solution near to the singularity is used as the initial solution for the numerical scheme. The method used in this paper is similar to that suggested in ref. [8], and is applied to equations (11) and (12) with modifications made to account for the associated derivative boundary conditions (13a). To remove the singularity experienced at $x = 0$, we introduce the variable ξ, which is related to x by the expression $\xi = x^{1/3}$ and all the graphical results presented are displayed in terms of this new variable ξ. As in Section 4, we now independently discuss the implications of the cases when there is no reactant consumption, $\lambda = 0$, and when the reactant consumption is included, $\lambda \neq 0$.

5.1. *Reactant consumption neglected*, $\lambda = 0$

In this section, we will investigate the behaviour of the numerical solution when $\lambda = 0$ for a range of values of ε. As seen in Section 4.1, taking $\lambda = 0$ implies that the dimensionless surface concentration remains at its ambient value, i.e. $\Phi_w \equiv 1$, along the entire surface. The numerical solution for the dimensionless wall temperature was obtained for $\varepsilon = 0.0$, 0.1, 0.2 and 0.3, with the results displayed in Fig. 1(a). We note that the behaviour of the solutions, for all values of ε considered, suggest that as $\xi \to \infty$ ($x \to \infty$) that the solutions do not approach constant values, but instead increase unbounded towards an infinite wall temperature. We also note that all the solutions exhibit a two-phase behaviour. The initial reaction phase starts at the ambient temperature extending along the surface away from the leading edge, progressing at a slow rate of increase in the temperature as we move along the surface. This behaviour continues, until at a finite distance along the surface, the rate of increase in the temperature rises sharply.

On considering the dimensionless temperature profiles for the case when $\lambda = \varepsilon = 0.0$, shown in Fig. 1(b), at various locations along the surface, ξ, as a function of the scaled distance away from the surface, η, the transition is further demonstrated. Through the work in Sections 3 and 4, we have found that $\eta = 14.0$ is the finite distance away from the surface that gives a very good approximation to an infinite distance away

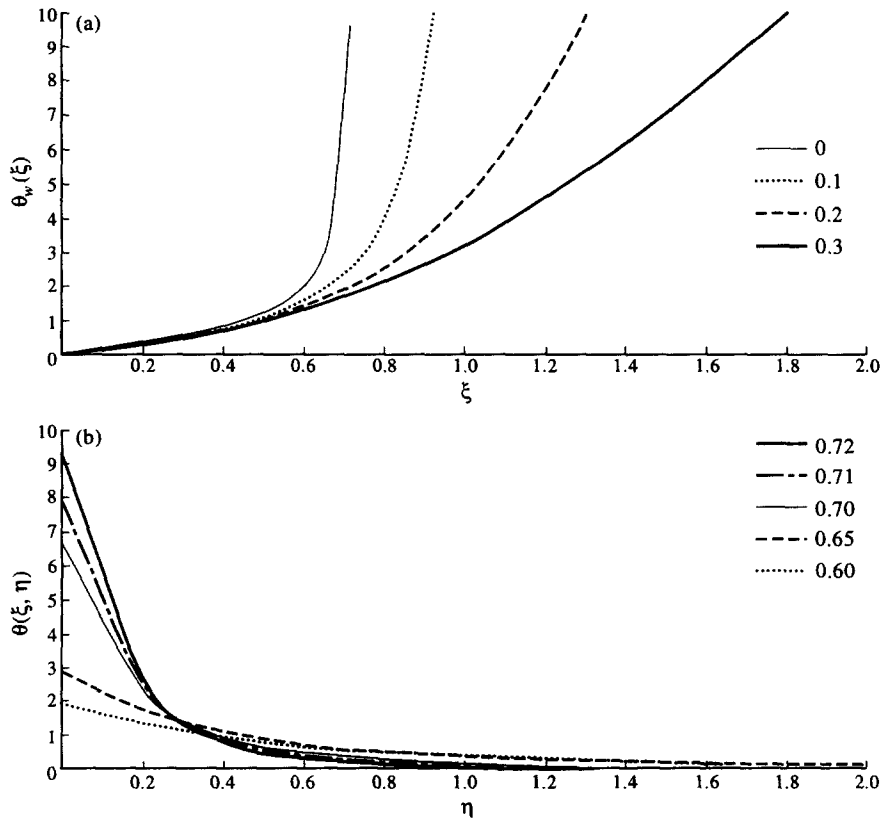

Fig. 1. (a) Graph of the dimensionless wall temperature θ_w plotted against $\xi = x^{1/3}$ for $\lambda = 0.0$, $\varepsilon = 0.0, 0.1, 0.2$ and 0.3; (b) graph of the dimensionless temperature profiles $\theta(\xi, \eta)$ plotted against η for $\lambda = 0.0$, $\varepsilon = 0.0$, at several locations along the surface $\xi = 0.60, 0.65, 0.70, 0.71$ and 0.72.

from the surface. Figure 1(b) has been truncated at $\eta = 2.0$ in order to clearly demonstrate the behaviour of the numerical solution at small distances from the surface.

In Fig. 1(b) we can see the sudden change in the dimensionless wall temperature as we move between $\xi = 0.65$ and 0.70 along the surface, thereby indicating the transitional region. Due to the Arrhenius kinetic model evoked in this paper, the rate of increase in the temperature correlates to an increase in the reaction rate, i.e. there is a transition from a slow reaction at low temperatures to a more vigorous reaction at higher temperatures. The characteristics of this transition phase are heavily dependent upon the value of ε considered. From Fig. 1(a) we can see that increasing the value of ε has the effect of increasing the value of ξ at which the transition begins to occur and also of limiting the rate of the temperature increase during the second phase. These features lead us to expect that, for a large enough value of ε, we would be unable to identify a transition period in the resulting smooth numerical solution.

5.2. *Reactant consumption included*, $\lambda \neq 0$

When reactant consumption is included in the problem, we investigate the effect upon the numerical solutions of varying one of the chemical parameters, λ or ε, whilst maintaining the other parameter at a constant value. The first case considered is where we fix $\varepsilon = 0.2$ and take $\lambda = 0.05$, 0.1 and 0.2. The numerical solutions for the dimensionless wall temperature and the dimensionless surface concentration are shown in Fig. 2(a, b), respectively.

As stated in equation (27), it is worthwhile noting at this stage to the relationship between the dimensionless wall temperature and the dimensionless surface concentration, for the case when $Le = 1$, i.e. $\Phi_w = 1 - \lambda\theta_w$. In Fig. 2(a), we observe that there exists a similar behaviour to that seen in Section 4.1. The numerical solutions for the dimensionless wall temperature exhibit the same two-phase behaviour, but instead of the temperature increasing indefinitely we see that at a finite distance along the surface that a third phase develops where the rate of increase in the temperature decreases and the dimensionless wall temperature approaches an asymptotic limit given by λ^{-1}. Corresponding to this the dimensionless surface concentration solutions, shown in Fig. 2(b), initially decrease rapidly away from the leading edge from the ambient concentration, $\Phi_w = 1$, and eventually decays to 0. These observations are in agreement with those made in Section 4.1, and we will investigate these correlations further in Section 6. We also note that for $\varepsilon = 0.2$ that the rate at which the concentration

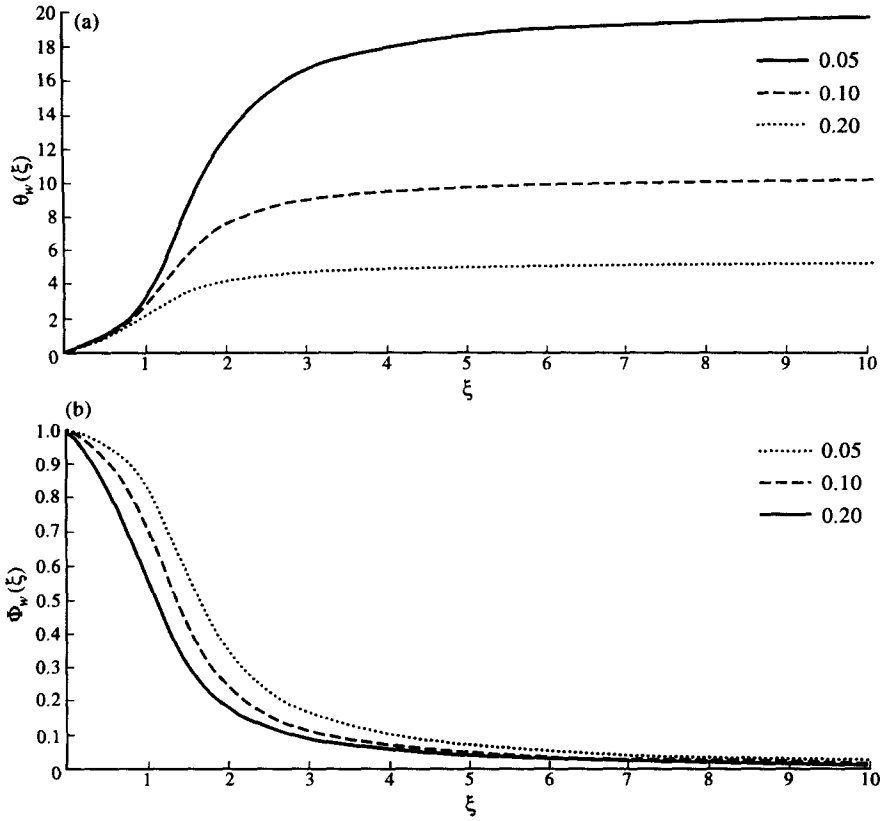

Fig. 2. (a) Graph of the dimensionless wall temperature θ_w plotted against $\xi = x^{1/3}$ for $\lambda = 0.05$, 0.1 and 0.2, $\varepsilon = 0.2$; (b) graph of the dimensionless surface concentration Φ_w plotted against $\xi = x^{1/3}$ for $\lambda = 0.05$, 0.1 and 0.2, $\varepsilon = 0.2$.

decreases has only a small dependence upon the value of λ.

We now investigate whether this observation holds when a larger range of values of λ is used, when $\varepsilon = 0.0$. We have calculated the numerical solutions when $\lambda = 0.2$, 0.5 and 1.0, with the results obtained are shown in Fig. 3. We again note that the asymptotic states which the dimensionless wall temperature solutions approach, as $\xi \to \infty$, are given by λ^{-1} and that the dimensionless surface concentration solutions decay to 0. For $\lambda = 0.5$ and 1.0 the rate of increase of the wall temperature and consequent decrease in the surface concentration is less pronounced than the solutions shown in Fig. 2.

We now consider the effect upon the numerical solutions for the dimensionless wall temperature and the dimensionless surface concentration of fixing the value of λ at 0.2 and taking $\varepsilon = 0.0$, 0.05, 0.1 and 0.2. The results for these cases are presented in Fig. 4. We observe that the numerical solutions for the dimensionless wall temperature and the dimensionless surface concentration approach the same asymptotic limits as $\xi \to \infty$, given by λ^{-1} and 0, respectively. In reference to equation (27), we observe how the solutions for the dimensionless wall temperature, as shown in Fig. 4(a), are 'mirrored' in the solutions for the dimensionless surface concentration, as shown in Fig. 4(b). The effects of varying the value of ε on the solutions for the dimensionless wall temperature in Fig. 4(a), are similar to those seen in Section 4.1, Fig. 1(a). In Section 4.1 we saw that decreasing the value of ε leads to a greater increase in the rate of temperature increase after the initial slow development of the reaction. This observation is also applicable to Fig. 4(b), where the smaller the value of ε the faster the reactant is depleted as we travel along the surface.

From the results presented in this section, we have seen that the smaller the value of ε, then the higher are the rate of increase and decrease of the dimensionless wall temperature and the dimensionless surface concentration, respectively, after the initial phase of the reaction at low temperatures. This behaviour of a rapid change, for small values of ε, can be reduced by increasing the value of λ, see Fig. 3, leading to a smoother transition between the initial reaction phase and the subsequent reaction phases.

6. COMPARISON BETWEEN SOLUTIONS

Finally, we now compare the similarity and asymptotic solutions, as derived in Sections 3 and 4, respectively, with the numerical solutions obtained in Sec-

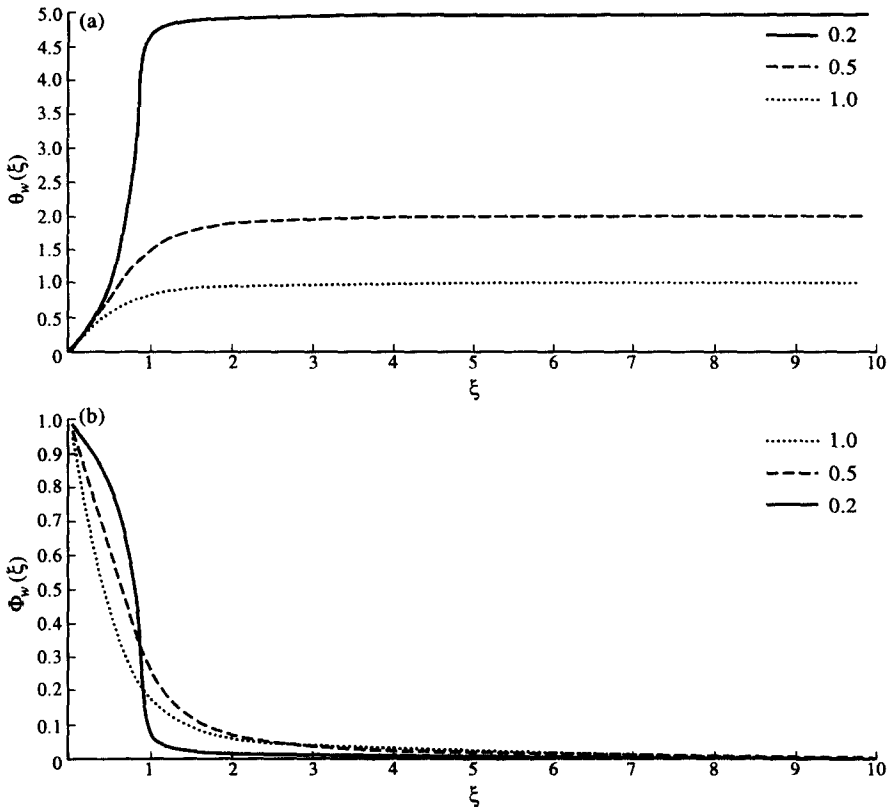

Fig. 3. (a) Graph of the dimensionless wall temperature θ_w plotted against $\xi = x^{1/3}$ for $\lambda = 0.2, 0.5$ and 1.0, $\varepsilon = 0.0$; (b) graph of the dimensionless surface concentration Φ_w plotted against $\xi = x^{1/3}$ for $\lambda = 0.2, 0.5$ and 1.0, $\varepsilon = 0.0$.

tion 5. Again we start by considering the case when no reactant is consumed during the progression of the reaction.

6.1. *Reactant consumption neglected*, $\lambda = 0$, $\varepsilon \neq 0$

In this section, no comparison is found between the dimensionless surface concentrations, since all the solutions, namely similarity, asymptotic and numerical, all return a constant value of 1, the value of the ambient concentration. Due to the nature of the asymptotic solutions derived in Section 4.1, we only need to compare the dimensionless wall temperature solutions for one specific case, since no solution which is valid for $x \gg 1$, when both $\lambda = 0.0$ and $\varepsilon = 0.0$, was derived. In order to illustrate the accuracy of the numerical solution we now compare the solutions for the dimensionless wall temperature when $\lambda = 0.0$ and $\varepsilon = 1.0$, with similar good comparisons being found for other values of $\varepsilon \neq 0$. The results are shown in Fig. 5, where logarithmic scalings have been used to make for a clearer comparison. Clearly we observe that the solutions are comparable in the regions were a correlation between the solutions was expected. The similarity solution, which is valid for $x \ll 1$, is in close agreement with the numerical solution for $x < 0.1$, with both solutions tending to 0 as $x \to 0$, and the asymptotic solution, valid for $x \gg 1$, agrees well with the numerical solution for $x > 10$ and as can be seen by comparing the results in Fig. 1(a) and equation (35a), for the numerical and asymptotic solutions, respectively; both solutions become linear in x as $x \to \infty$.

6.2. *Reactant consumption included*, $\lambda \neq 0$

We now make the comparison between solutions for the case when $\lambda = 0.1$ and $\varepsilon = 0.2$, with similar good comparisons found for other combinations of values of λ and ε. The results for the dimensionless wall temperature and the dimensionless surface concentration solutions are shown in Fig. 6(a, b), respectively. For this comparison a logarithmic scaling was only used to scale the x values, thereby producing a clear picture of the solutions' behaviour. Clearly in Fig. 6(a, b), there are definite correlations between the similarity and numerical solutions for $x < 0.01$ and between the asymptotic and numerical solutions for $x > 100$. For this case, where the reaction consumes reactant as it progresses along the surface both the dimensionless wall temperature and the dimensionless surface concentration solutions have steady state solutions at both limits of the plate, i.e. at $x = 0$ and $x = \infty$, given by:

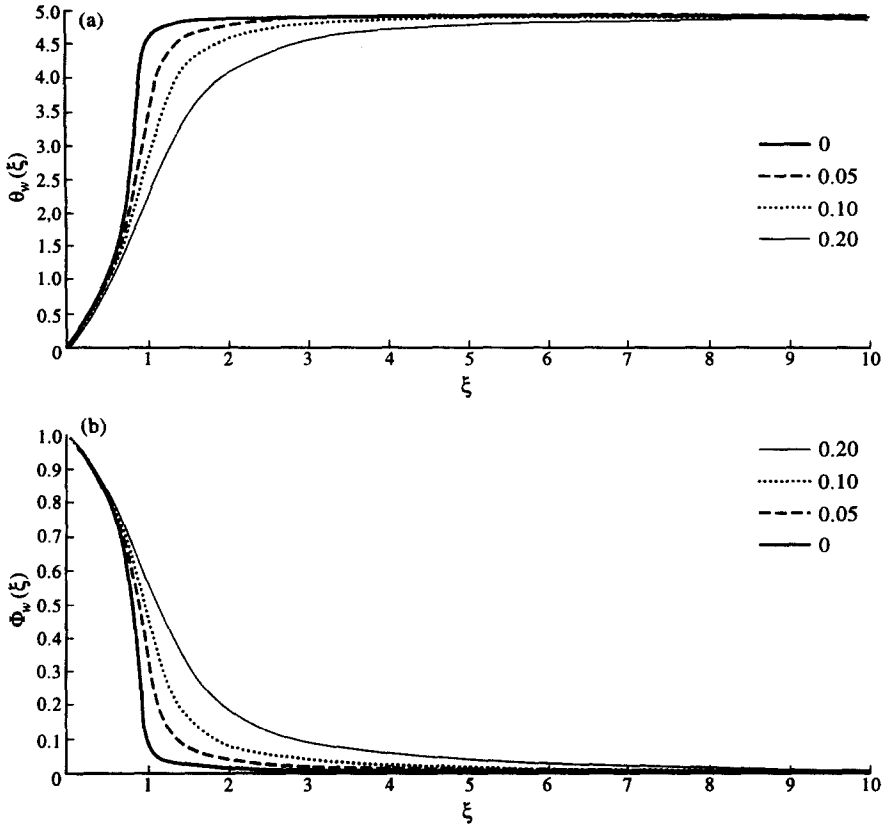

Fig. 4. (a) Graph of the dimensionless wall temperature θ_w plotted against $\xi = x^{1/3}$ for $\lambda = 0.2$, $\varepsilon = 0.0$, 0.05, 0.1 and 0.2; (b) graph of the dimensionless surface concentration Φ_w plotted against $x = \xi^{1/3}$ for $\lambda = 0.2$, $\varepsilon = 0.0$, 0.05, 0.1 and 0.2.

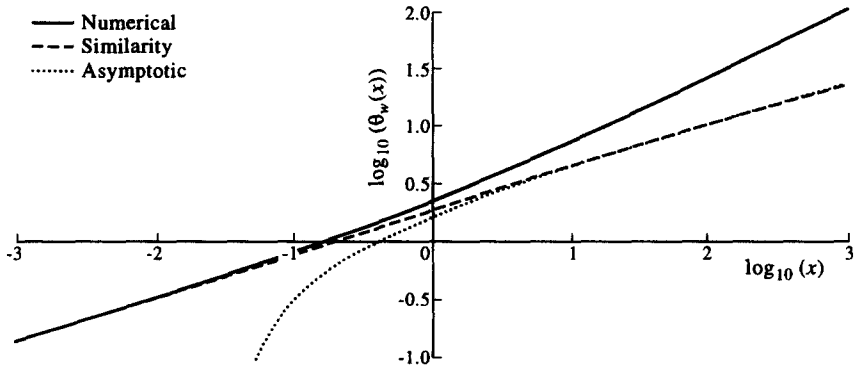

Fig. 5. Graph of a function of the dimensionless wall temperature solutions, $\theta_w(x)$ plotted against a function of x for $\lambda = 0.0$, $\varepsilon = 1.0$.

$$\theta_w(0) = 0, \quad \Phi_w(0) = 1,$$
$$\theta_w(\infty) = \lambda^{-1}, \quad \Phi_w(\infty) = 0. \qquad (51)$$

These steady state solutions are clearly attained by all the solutions, where applicable, as demonstrated in Fig. 6(a, b).

7. DISCUSSION

The free-convection boundary-layer flow on a semi-infinite, vertical catalytic surface which is embedded in a porous media, driven by an exothermic reaction on the surface, has been considered. Initially the reaction occurs on the surface, with the heat generated being conducted away into the surrounding fluid. This results in a natural convective flow within the porous media, which influences the temperature of the surface and, hence, the progression of the reaction. This mechanism in turn controls the rate of reactant consumption, whilst the convective flow introduces more reactant to the surface drawn from the surrounding fluid.

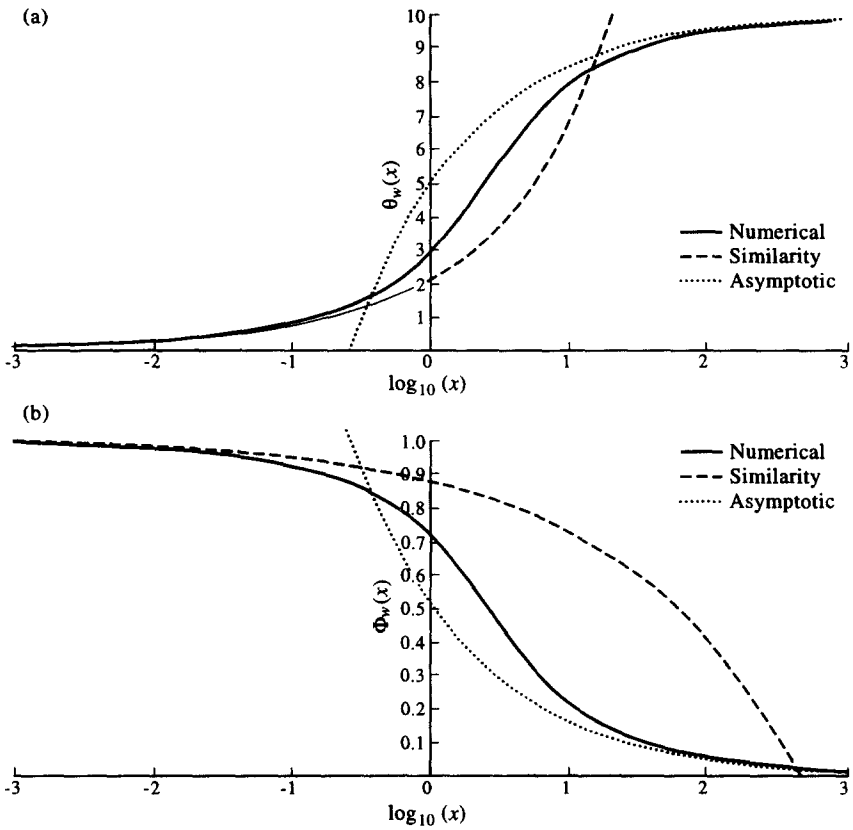

Fig. 6. (a) Graph of the dimensionless wall temperature solutions, $\theta_w(x)$ plotted against a function of x for $\lambda = 0.1$, $\varepsilon = 0.2$; (b) graph of the dimensionless surface concentration solutions, $\Phi_w(x)$ plotted against a function of x for $\lambda = 0.1$, $\varepsilon = 0.2$.

The reaction has been modelled as first-order exothermic reaction using Arrhenius kinetics. The Darcy–Boussinesq approximation has been invoked, which had the advantage of simplifying the flow under consideration. By assuming the validity of the boundary-layer approximation, it was found that the temperature of the system and the concentration of the reactant could be modelled by solving a pair of coupled, parabolic partial differential equations subject to the associated boundary conditions.

Similarity solutions for the dimensionless wall temperature and surface concentration were obtained which are valid near to the leading edge of the catalytic surface. These were complemented by asymptotic solutions for the dimensionless wall temperature and surface concentration which are valid far from the leading edge of the catalytic surface. Two distinct sets of asymptotic solutions were obtained for two independent cases, namely when the reactant consumption was neglected and when the reactant consumption was included.

The full numerical solutions of the governing partial differential equations exhibited a behaviour which is strongly dependent upon the values of the chemical parameters λ and ε. It was seen for the case when $\lambda = 0.0$ that the numerical solution has a two-phase behaviour comprising of an initial slow reactive state occurring at low temperatures followed by a period of transition to a more reactive state occurring at higher temperatures with reaction progress indefinitely leading to an infinite wall temperature. For the cases when temperature $\lambda \neq 0$ this two-phase behaviour was limited by another period of transition where the rate of reaction decreased and the temperature attained a steady state, given by λ^{-1}, due to the depletion of the reactant. The changes occurring between these phases were less distinct when higher values of ε and/or λ are used in generating the numerical solutions.

These numerical solutions were then compared to the similarity and asymptotic solutions, where applicable, and regions of agreement between the solutions were located for the cases considered. Within these limits the similarity and asymptotic solutions, where applicable, should be used, with the numerical solution used between these limits when attempting to generate a solution to the problem discussed herein.

Acknowledgements—B. J. Minto would like to thank the EPSRC and the Centre for Computational Fluid Dynamics for their financial support.

REFERENCES

1. Nield, D. A. and Bejan, A., *Convection in a Porous Media*, Springer, Berlin, 1992.

2. Cheng, D. and Minkowycz, W. Y., Free-convection about a vertical flat plate embedded in a porous medium with application to heat transfer from a disk. *Journal of Geophysics Research*, 1977, **82,** 2040–2044.
3. Kordylewski, W. and Krajewski, Z., Convection effects on thermal ignition in porous media. *Chemical Engineering Science*, 1984, **39,** 610–612.
4. Vilijoen, H. and Hlavacek, H., Chemically driven convection in a porous medium. *A.I.Ch.E. Journal*, 1987, **39,** 1344–1350.
5. Chen, Y. K., Hsu, P. F., Lim, I. G., Lu, Z. H., Matthews, R. D., Howell, J. R. and Nichols, S. P., Experimental and theoretical investigation of combustion within porous inert media. Poster Paper, *Twenty-Second International Symposium on Combustion*, 1988, pp. 22–207.
6. Hsu, P. F., Howell, J. R. and Matthews, R. D., A numerical investigation on premixed combustion within porous inert media. Poster Paper. *ASME/JSME Meeting*, 1991, Las Vegas, Nevada.
7. Chao, B. H., Cheng, P. and Le, T., Free-convective diffusion flame sheet in porous media. *Combustion Science Technology*, 1994, **99,** 221–234.
8. Chao, B. H., Wang, H. and Cheng, P., Stagnation point flow of a chemically reactive fluid in a catalytic porous bed. *International Journal of Heat and Mass Transfer*, 1996, **39,** 3003–3019.
9. Chaundhary, M. A. and Merkin, J. H., Free-convection stagnation-point boundary-layers driven by catalytic surface reactions: I the steady states. *Journal of Engineering Mathematics*, 1994, **28,** 145–171.
10. Merkin, J. H. and Chaundhary, M. A., Free-convection boundary layers on vertical surfaces driven by an exothermic surface reaction. *Quarterly Journal of Mechanics and Applied Mathematics*, 1994, **47,** 405–428.
11. Mahmood, T. and Merkin, J. H., Mixed convection on a vertical circular cylinder. *Journal of Applied Mathematics and Physics* (*ZAMP*), 1988, **39,** 186–203.
12. Rees, D. A. S. and Pop, I., Free convection induced by a vertical wavy surface with uniform heat flux in a porous medium. *Journal of Heat Transfer*, 1995, **117,** 547–550.
13. Merkin, J. H. and Zhang, G., The boundary-layer flow past a suddenly heated vertical surface in a saturated porous medium. *Warme-und Stoffubertragung*, 1992, **27,** 299–304.
14. Wright, S. D., Ingham, D. B. and Pop, I., On natural convection from a vertical plate with the prescribed surface heat flux in porous media. *Transport in Porous Media*, 1996, **22,** 183–193.